J. Mt. Sci. (2021) 18(3): 635-645 e-mail: jms@imde.ac.cn http://jms.imde.ac.cn
https://doi.org/10.1007/s11629-020-6475-7

Original Article

Using thermal remote sensing in the classification of mountain permafrost landscapes

Svetlana V. KALINICHEVA* https://orcid.org/0000-0002-0544-8395; e-mail: ikoveta@rambler.ru

Alyona A. SHESTAKOVA https://orcid.org/0000-0002-0648-0362; e-mail: aashest@mail.ru

** Corresponding author*

Melnikov Permafrost Institute, Siberian Branch of Russian Academy of Sciences, Yakutsk677010, Russia

Citation: Kalinicheva SV, Shestakova AA (2021) Using thermal remote sensing in the classification of mountain permafrost landscapes. Journal of Mountain Science 18(3). https://doi.org/10.1007/s11629-020-6475-7

Abstract: Thermal infrared satellite imagery is increasingly utilized in permafrost studies. One useful application of the land surface temperature (LST) products is classification and mapping of landscapes in permafrost regions, as LST values can help differentiate between frozen and unfrozen ground. This article describes a new approach to the use of LST. The essence of the new approach lies in the fact that in the territory where it is impossible to determine (indicate) the state of the underlying ground according to the same morphological characteristics (relief, vegetation, soil composition, etc.), the LST parameter, which reflects the thermal state of the landscape, allows as an additional criterion (indicator) identify frozen / un-frozen landscapes. In this work, using the above approach, a map has been compiled, which shows the permafrost natural-territorial complexes of the Elkon Massif, Eastern Siberia, including topography, slope aspect, slope angle, vegetation, snow cover and LST. The map provides a more detailed and updated description of permafrost distribution in the study area.

Keywords: Permafrost mapping; Permafrost landscape classification; Landsat; Thermal infrared imagery; Mountain permafrost; Land surface temperature; Eastern Siberia.

Received: 18-Sep-2020
Revised: 28-Dec-2020
Accepted: 29-Jan-2021

1 Introduction

Permafrost, which occupies 25% of the world's land, is highly sensitive to climate warming and human activities. Permafrost degradation decreases the stability of landscapes and can trigger widespread development of many destructive processes. Therefore, monitoring and mapping of permafrost conditions are of high priority today. Monitoring the thermal state of permafrost using ground-based measurements is challenging due to the great extent of permafrost terrain, poor accessibility, and limited number of boreholes. Where field data is unavailable, remote sensing becomes a dominant tool. In particular, the Land surface temperature (LST) measured from satellites is an important parameter for monitoring and mapping the heat balance of permafrost areas.

The LST shows the thermal state of the surface and is one of the key parameters in the physics of land surface processes, combining surface-atmosphere interactions and the energy fluxes between the atmosphere and the ground (Marchenko et al. 2009). It provides a more direct indicator for the occurrence of permafrost and should be used in permafrost mapping (Nelson and Outcalt 1987; Hachem 2009).

Thermal infrared sensing which produces LST data is a relatively recent technique which has been applied to permafrost studies since the 1970s (Greene

1971, 1972; Leshack et al. 1972; Leshack and Morse 1973). Kudryavtsev et al. (1979) included thermal infrared sensing into the list of remote geophysical techniques applicable to frozen ground studies. A description of the method was presented by Nekrasov (1979) in his brief review of aerial and space-borne techniques and their potential for permafrost studies. He wrote that the most informative were infrared images for they proved valuable for determining the temperature field of the underlying surface. In later years, significant progress was noted in the description and application of the thermal remote sensing method in permafrost research and mapping. The development of this method is probably associated with the satellite systems development with thermal sensors, as well as the possibility to supplement or replace (to some extent) with LST data the missing field data in monitoring and mapping the permafrost. The latter is related to the relationship between LST and field data (in-situ) established by researchers.

The land surface temperature (LST) is retrieved available through a number of sensors, ranging from low (e.g., MODIS, AATSR, AVHRR) to medium (e.g., LANDSAT, ASTER) spatial resolution. The first regular satellite surveys of the thermal properties of the land surface began to be carried out since the 1970s by the NOAA AVHRR scanning system in a spatial resolution of 1.1 km and a temperature resolution of 0.1°C-0.2°C, a little later by the Terra/Aqua MODIS radiometer also in a low spatial resolution of 1 km. The MODIS spectroradiometer became essentially the successor of the AVHRR, in comparison with which it had significantly improved spectral and radiometric resolution, mutual geometric referencing of spectral channels, and absolute radiometric calibration (Garbuk and Gershenzon 1997). MODIS is one of the key survey device installed on board the American satellites «Terra» (in orbit since 1999) and «Aqua» (in orbit since 2002), conducting Earth exploration from space, under the EOS (Earth Observing System) program of the USA National Aerospace Agency (NASA). The distinctive features of AVHRR and MODIS satellite images are the high frequency of information updates (up to 2 times a day), global coverage of territories (about 3000 km) and low resolution on the terrain (about 1 km). The «Terra» satellite also has an ASTER multispectral radiometer, which conducts thermal infrared survey in 5 spectral ranges with a spatial resolution of 90 m. The multispectral of the device allows accurate recording of the land surface temperature and decryption of the main types of ground (Handbook 1999). As part of the Landsat (USA) long-term program for the study of Earth's natural resources, the satellites «Landsat-5» (in 1984) and «Landsat-7» (in 1999) were launched into orbit, conducting thermal surveys with a resolution of 120 m and 60 m, respectively (Handbook 2019). For the first time, at a sufficiently detailed level, satellite data from the Landsat series spacecraft made it possible to obtain heat maps of most of the land surface, and many regions were shot many times. Landsat satellites have been a valuable source of remote sensing data for medium-scale geographic research for many years (Kravtsova et al. 2012). Landsat imagery has a unique combination of coverage, spatial resolution and radiometric accuracy. From the point of view of the remote sensing information content, the existing space systems allow thermal survey on a global (AVHRR, MODIS) and regional (TM, ETM +, TIRS, ASTER) scales. Although thermal infrared space systems are characterized by huge capabilities - high visibility, high penetrability, etc., however, there are limitations for satellite data, for example, their dependence on weather conditions (cloud cover makes thermal survey impossible). The latter has some difficulties in filling the LST data gaps. In view of this, various researchers offer options for solving this issue. For example, Langer et al. (2010) and Westermann et al. (2011) investigated the spatial and temporal variability of summer LSTs using a high resolution ground-based thermal imaging system at a polygonal tundra site in northern Siberia (Russia) and High Arctic tundra in Svalbard (Norway). Langer et al. (2010) noted that cloudy conditions might lead to displacement weekly mean temperatures which was inferred from MODIS LST data, and recommended a solution to improve the accuracy of mean LST values by combining cloud cover information with a gap-filling procedure. Westermann et al. (2011) concluded that a reliable gap-filling procedure to moderate the effects of long cloudy periods would be of great importance for future LST-based permafrost monitoring schemes. Some solutions for the gaps filling are given in Hachem et al. (2009, 2008, 2012), Ran et al. (2015), etc.

A number of studies have been undertaken to establish relationships between ground-based (in-situ) data and LST values. It should be noted, however,

that approaches used vary significantly. For example, the MODIS Aqua/Terra LST product is used by some authors, while others utilize the LANDSAT LST or ASTER Terra LST. The choice of a particular product is dictated by the objectives of the research undertaken. One further difference is the time frame selected: some studies use LST data for a multi-year period (for all seasons) (e.g., Marchenko et al. 2009; Hachem 2009; Westermann et al. 2015; Gisnås et al. 2013; Zhao et al. 2017; Shi et al. 2018), while others select the period of maximum land-surface temperature contrasts (summer-autumn) (e.g., LeShack and Morse 1973; Nekrasov 1979; Kornienko 2007; Kornienko 2012; Medvedkov 2016; Kalinicheva et al. 2019). The choice of time frame is also determined by the purposes and tasks of the study. Continuous LST series are mainly used for monitoring and modeling the spatial distribution of permafrost, while a specific time period is better suited for distinguishing between frozen and unfrozen ground.

LST correlations with different variables have been obtained, including air temperature and ground surface temperature (Makarov 2017; Luo et al. 2018; Li 2019), active-layer temperature (Kornienko 2007; Kornienko 2012), and ground temperature at the depth of zero annual amplitude (ZAA temperature) (Kalinicheva et al. 2019). Several studies considered the possibility of delimiting permafrost boundaries based on annual time series of ground surface temperature and its correlation with LST (Hachem 2009, Hachem et al. 2008). These studies were based on the relationship between the mean annual ground surface temperature and the permafrost temperature (Smith 2002; Sazonova and Romanovsky 2003).

Of special interest are studies that attempted to relate the ground condition (frozen or unfrozen) and LST values. For example, Kornienko (2007, 2012) explored the utility of thermal remote sensing in permafrost monitoring for tundra and fire-affected landscapes in western Yamal. The author concluded that LST was useful in characterizing the thermal condition of frozen ground. Based on multi-temporal images from Landsat-7, NOAA satellites for snow-free summer-autumn months and field observations, ice-poor permafrost with deep active-layer thaw was found to be associated with high LST values, while ice-rich ground with a shallow active layer to show low LST values.

There is growing interest in using LST in modeling permafrost temperature. For example, Marchenko et al. (2009) presented modeling of permafrost and active layer inhomogeneities (using the GIPL-1.1 model) based on the MODIS LST scanner data and meteorological observations at key areas in Northern Eurasia.

Westermann et al. (2015) and Gisnas et al. (2013) made an attempt to model the temperature regime of permafrost in the North Atlantic region, based on data from the MODIS thermal infrared survey for a 10-year period (2003-2012). Modeling was performed with account for air temperature and snow cover. Modeling results were compared with ground temperature measurements from 143 boreholes in western Russia, northern Europe and Canada and showed a good agreement with field data. As part of the modeling study, maps of ground temperature and permafrost distribution were produced at a spatial scale of 1 km.

A few studies were undertaken to model the spatial distribution of permafrost on the Qinghai-Tibet Plateau using MODIS LST. For example, Zhao et al. (2017) used several models, three of which incorporated ten-year LST data (2003-2012) as a parameter for ground surface temperature. Modeling results were validated against existing permafrost maps and field data from three representative sites. Although the models overestimated permafrost distribution, the authors believe that, compared to empirical models, the LST-based models give better results for island permafrost in the southern Qinghai-Tibet Plateau. Shi et al. (2018) compiled a permafrost distribution map of the Qinghai-Tibet Plateau using MODIS satellite images with a resolution of 1 km and assessing several variables, such as elevation, vegetation cover, soil moisture, and land surface temperature according to LST.

This article presents a brief overview of the development of thermal infrared sensing for permafrost applications. It is not intended to present LST estimation methods or compare satellite capabilities. The list of LST studies referred to in this review is not all-inclusive.

If we talk about the prospects of using LST, then the most promising areas of LST application, in our opinion, are monitoring of changes in permafrost under climate change, thermal soil modeling and assessment of landscape stability. In addition, LST can provide a useful aid in improving permafrost-landscape classifications. Landscape studies of permafrost are now widely used in permafrost

mapping to study the dynamics and evolution of permafrost, including problems caused by current climate warming (Jorgenson et al. 2014, 2018; Kokelj 2017; Wang et al. 2019). Classification and mapping of permafrost and landscape are necessary to study trends in the development of the natural environment in the northern and highland regions of permafrost. The cryogenic factor in the permafrost zone plays a leading role in the differentiation of landscapes, so it was necessary to consider during classification constructions (Fedorov 1991).

Despite continuous improvements in permafrost-landscape classification, there are areas where the subsurface thermal condition is difficult to infer only using surface characteristics, such as topography, vegetation, soil or rock type, etc. In other words, similar morphological landscape characteristics can be found in areas of both frozen and unfrozen ground. In this case, the LST parameter which reflects the thermal state of the landscape, can serve as an additional criterion (indicator) for the identification of frozen/unfrozen landscapes. From this point of view, LST can significantly improve the existing traditional permafrost-landscape classifications. Despite the relevance of this application of LST, there is currently no research (scientific work) in this area. As a first step in this direction, we developed a classification of permafrost landscapes for the Elkon Massif, a mountainous area in Eastern Siberia.

2 Materials and Methods

The study area is located in southern Yakutia between latitudes 58°24' and 58°48'N and longitudes 125°45' and 126°36'E. Permafrost conditions in the Elkon Massif are relatively well known owing to its economic significance and high mining potential.

Ground-based data (temperature measurements available from 45 boreholes) and satellite imagery were used in mapping and classification. A detailed description of the source data, satellite image processing methods, and general environmental characteristics of the study area was given in Kalinicheva et al. (2019). The basic principles for identifying and mapping permafrost landscapes were presented by Fedorov et al. (2018).

A thermal image (LST) best suited for the area of interest was selected based on the analysis of a series of Landsat-5/TM and Landsat-8/TIRS satellite imagery for the period from 2000 to 2015. The analysis of different thermal images for various seasons (months) with field data showed correlation of LST with ZAA temperature (commonly measured at depths of 10–25 m) only between late August and early September (Kalinicheva et al. 2019). Therefore, a Landsat-5/TM thermal satellite image acquired on August 21, 2009 was selected because of the absence of interference (cloudiness, etc.) and a high correlation with the temperature of the underlying ground (R^2 = 0.83) (Fig.1).

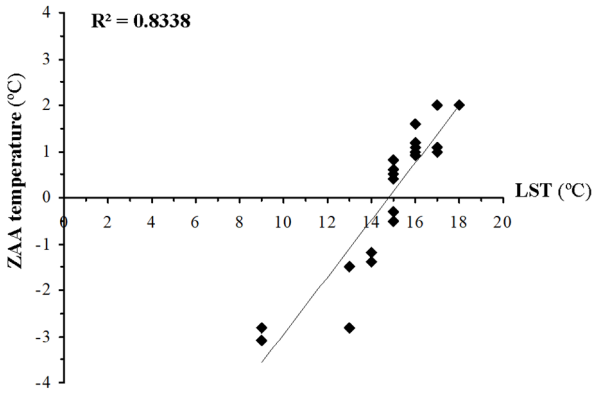

Fig. 1 Correlation analysis between land surface temperature (LST, °C) and ground temperature at the depth of zero annual amplitude (ZAA temperature, °C) of the Elkon mountain at the end of August, 2009.

The good correlation between LST and ZAA temperature in the second half of August to the first half of September is likely due to the fact that the active layer in the study area reaches its maximum depth and the seasonally frozen layer thaws completely during this period. In addition, the masking influence of actively growing vegetation is excluded and abnormal temperature contrasts due to solar heating are minimal. A similar opinion on the choice of the period for identifying frozen and unfrozen ground was given by Nekrasov et al. (1979), Leshack (1973) and Kornienko (2007, 2012).

3 Results

From the satellite imagery selected (dated August 21, 2009), the LST variability range from 9°C to 26°C was obtained for the Elkon Massif at the time of satellite overpass (Fig. 2).

The analysis of the LST map (Fig. 2) along with the field data shows that, all other factors being equal, the intensity of LST in permafrost areas is generally

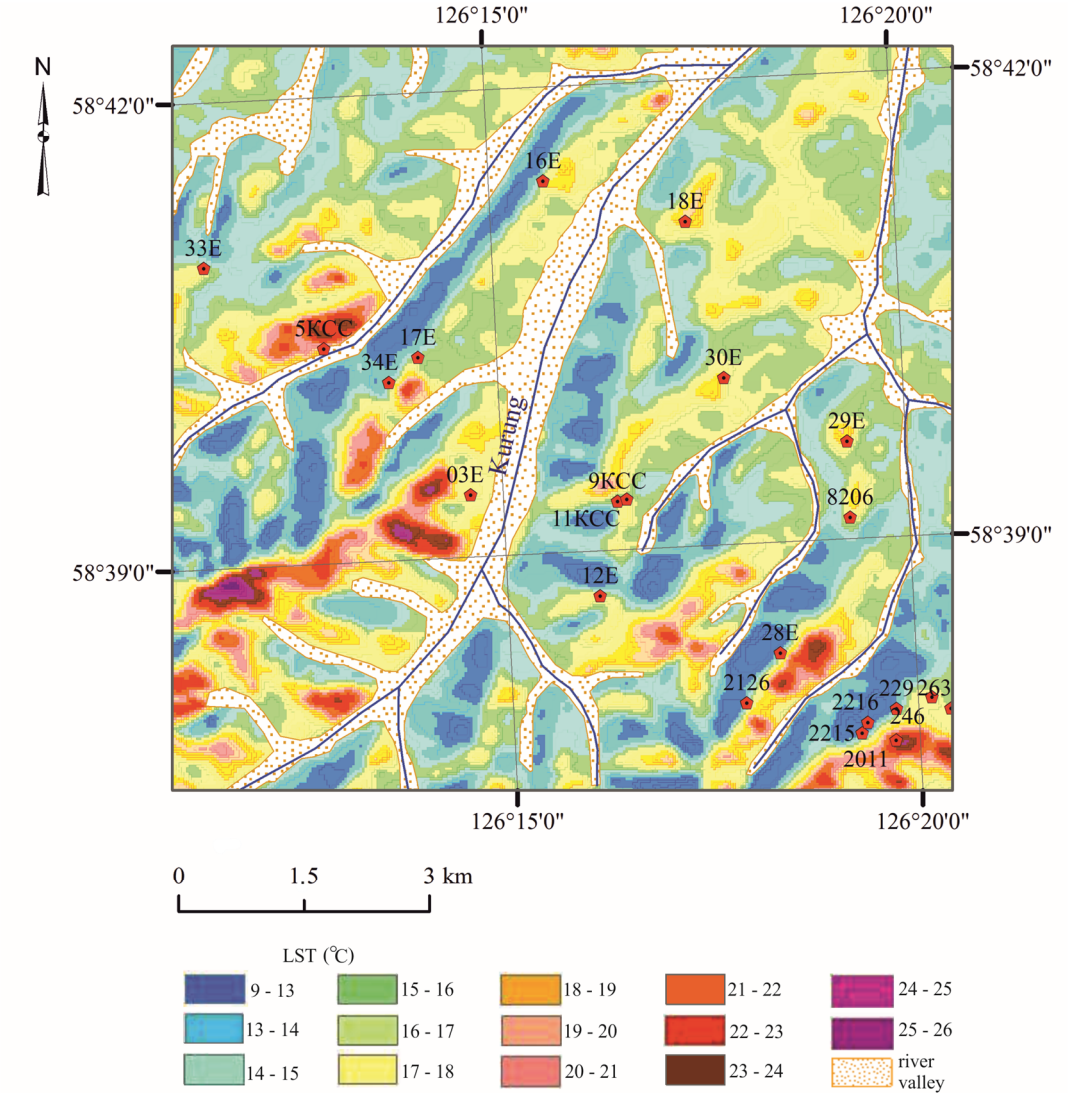

Fig. 2 Map of land surface temperature (LST, °C) of the Elkon Massif, 21 August 2009. Numbered dots represent geothermal borehole ID.

lower (9°C–15°C) than in landscapes on unfrozen ground (16°C–19°C). However, in the areas with rock debris and stone streams, LST in summer is higher than in unfrozen ground (17°C–26°C). The reason for this is that areas with exposed rock heat up more than those covered with vegetation.

Classification of permafrost landscapes was carried out in the process of mapping by overlaying separate layers - topography, vegetation, snow cover, and LST in the ArcGIS 10.1 program (ESRI (Environmental Systems Research Institute), Redlands, California, USA). The essence of permafrost mapping is sequential mapping and refinement of boundaries according to selected environmental factors.

Classification consisted of two stages. At the first stage, a classification of the natural-territorial complexes in the study area was compiled, which included such surface variables as topography, aspect and surface slope (stratigraphic-genetic complexes), as well as plant association types (Section 3.1). The combination of topography and vegetation provides the basis for landscape mapping (Sochava 1978). This principle is used by many researchers to differentiate and map permafrost-landscape categories (e.g., Fedorov et al. 2018).

At the second stage, identification of permafrost conditions was carried out for selected natural-territorial complexes based on snow depth and LST (Section 3. 2). Snow-depth maps were superimposed on the landscape base (combination of topography and vegetation), specifying the conditions for ground

freezing and permafrost formation. Further, overlaying of the LST map refined the state of the landscapes, differentiating between frozen and unfrozen ground.

3.1 Classification of natural-territorial complexes (stage 1)

In this study, we considered near-watershed and slope landscapes with discontinuous permafrost occurring at elevations between 700 and 1200 m. In view of this, when compiling the classification on the indicated altitude segment, near-watershed and slope landscapes were distinguished separately from each other. Thus, in the table, near-watershed landscapes were identified by the capital letter "A", and slope landscapes by the letter "B".

Eight slope aspects (north, northwest, west, southwest, south, southeast, east, and northeast) were considered which were later combined into 3 aspect groups: windward (north and northwest), transitional (west and northeast) and leeward (east, southeast, south and southwest) according to microclimatic similarity and prevailing winds. Aspect groups in the classification table were marked with Roman numerals: I - windward; II - transitional; III - leeward.

The nature of the stratigraphic-genetic complexes is associated with surface slope. Thus, residual and slopewash deposits, consisting of bouldery and gravelly material with sand and sandy silt, are characteristic of gentle slopes (0°-10°), slopewash-colluvial deposits, represented by sandy loams, sands with gravel and fine gravel, occur on the moderate slopes (10°-15°), and colluvial deposits, characterized by bouldery and gravelly material with sandy loam and sandy aggregate, are common on steep slopes (15° and higher). In the table, these stratigraphic-genetic complexes were identified by means of numbers: 1 - gentle slopes (0°-10° on residual and residual-slopewash deposits), 2 - moderate slopes (10°-15° on slopewash-colluvial sediments) and 3 - steep slopes (15° < on colluvial deposits).

The types of vegetation cover were indicated in capital letters: larch forests (a), larch forests with pine (b), pine-larch forests (c), sparse larch forest with mountain pine thickets (d), open larch forest with alder and mountain pine thickets (e), mountain pine thickets (f), sparse mountain pine forest with rock debris patches (g) and stone fields (with lichen) (h).

By overlaying the above environmental (landscape) factors, a new layer was obtained - natural-territorial complexes (NTC) (Fig. 3).

In Table 1, natural-territorial complexes were first identified by a combination of factors (for example, AI1b, AI1d, etc.), and further, each combination was assigned a digital identifier from 1 to 119. The application of these layers made it possible to obtain 119 new units - types of NTC in the study area.

3.2 Classification of permafrost natural-territorial complexes (stage 2)

At the second stage, as mentioned above, the

Table 1 Natural-territorial complexes in the Elkon Massif. (Fragment)

Topography	Slope orientation		Stratigraphic-genetic complexes	Vegetation cover	NTC	ID
	Aspect	Wind direction				
Near-watershed slopes and watersheds (A)	North/ north-west	Windward (I)	e, ed (1)	Larch forests with pine and mountain pine thickets (b)	AI1b	1
				Sparse larch forest with mountain pine thickets (d)	AI1d	2
				Open larch forest with alder and mountain pine thickets (e)	AI1e	3
				Mountain pine thickets (f)	AI1f	4
				Sparse mountain pine forest with rock debris patches (g)	AI1g	5
				Stone fields (with lichen) (h)	AI1h	6
			dc (2)	Larch forests with pine and mountain pine thickets (b)	AI2b	7
				Sparse larch forest with mountain pine thickets (d)	AI2d	8
				Open larch forest with alder and mountain pine thickets (e)	AI2e	9
				Mountain pine thickets (f)	AI2f	10
				Sparse mountain pine forest with rock debris patches (g)	AI2g	11
				Stone fields (with lichen) (h)	AI2h	12
			c (3)	Larch forests with pine and mountain pine thickets (b)	AI3b	13
				Sparse larch forest with mountain pine thickets (d)	AI3d	14
				Mountain pine thickets (f)	AI3f	15
				Sparse mountain pine forest with rock debris patches (g)	AI3g	16
				Stone fields (with lichen) (h)	AI3h	17

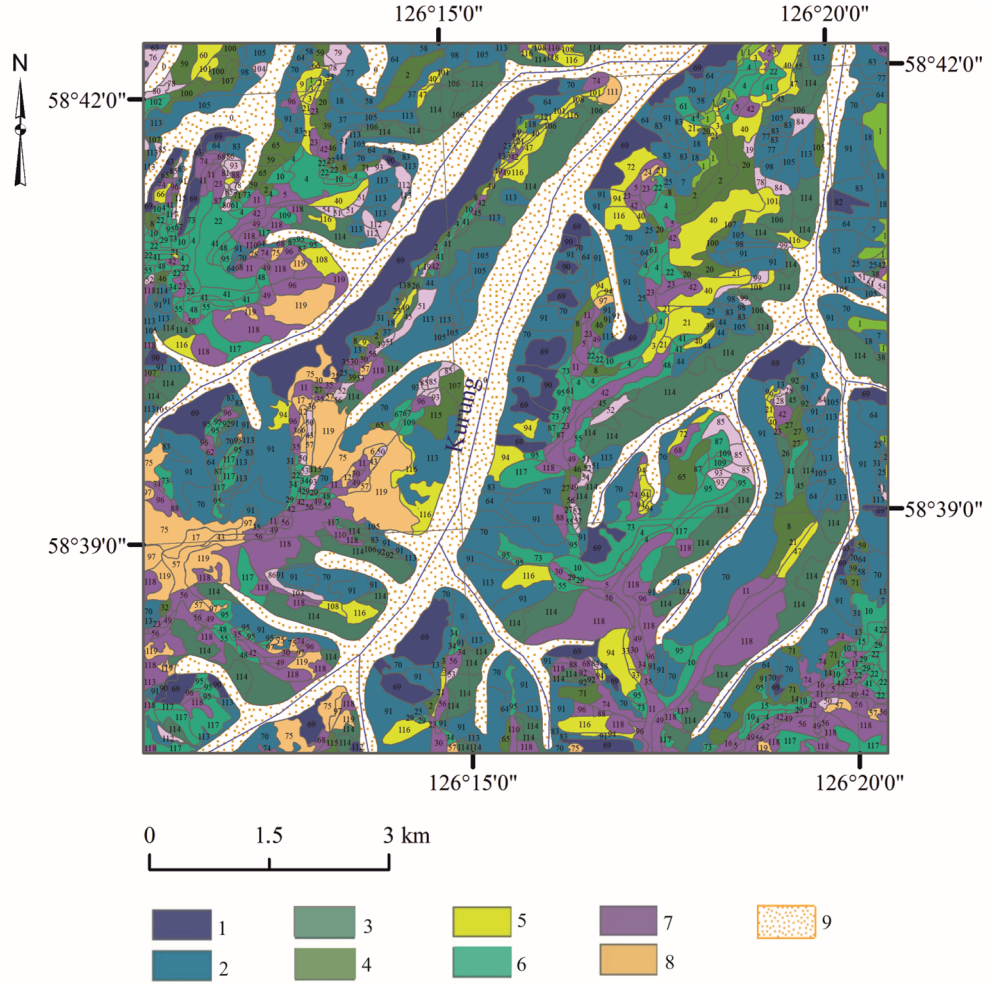

Fig. 3 Map of types of natural-territorial complexes of the Elkon Massif. The types of vegetation cover are highlighted in color: 1. larch forest; 2. larch forests with pine; 3. pine-larch forests; 4. sparse larch forest with mountain pine thickets; 5. open larch forest with alder and mountain pine thickets; 6. mountain pine thickets; 7. sparse mountain pine forest with rock debris patches; 8. stone fields (with lichen); 9. river valley. The numbers on the map indicate the types of natural-territorial complexes (explanations are given in Table 1).

NTC types were differentiated based on snow depth and LST. To compile the final permafrost-landscape map, the maps of snow depth and LST were superimposed on the NTC map.

The overlaying of these layers made it possible to obtain 185 new units, here referred to as 'types of permafrost natural-territorial complexes' (1174 polygons) (Fig. 4).

In the indication table (Table 2), the first 2 columns indicated the NTC - description and identification number. The third column shows the LST value of a landscape. The LST intervals that identify frozen and unfrozen ground as well as ground with temperatures about 0°C are described above. The ground condition, based on the LST values, was designated by Latin letters - A, B, C, D. The snow thickness is shown in the last column of the table.

This article presents a fragment of a large table of the improved classification of permafrost natural-territorial complexes on the example of landscapes of windward (northern, northwestern) aspects on gentle slopes. As can be seen from the above fragment, in the same types of landscapes (for example, mountain pine thickets on the gentle slopes of windward (northern, northwestern) aspects), the underlying ground can be both frozen and unfrozen. One of the factors influencing the condition of the ground, as shown in the last column, is snow cover. The role of the LST parameter is that it identifies the condition of the ground. This is what distinguishes the traditional classification of permafrost landscapes from this improved one using LST.

As is known, deep snow cover has a warming effect on the underlying ground. This effect is evident

Table 2 Types of permafrost natural-territorial complexes of the Elkon Massif.
(Fragment, on the example of windward landscapes (northern, north-western aspects on gentle slopes)

Landscape			LST	Symbol with LST	Ground condition	General symbol	Snow cover(cm)
Description		Id					
Landscapes of near-watershed sites	Larch forests with pine, mountain pine thickets on near-watershed sites (700-900 m) of windward (northern, northwestern) aspects on gentle slopes	1	9-15	A	Frozen	1A	<80
			15-16	B	Transitional	1B	80-100
	Sparse larch forest with mountain pine thickets on near-watershed sites (750-900 m) of windward (northern, northwestern) aspects on gentle slopes	2	9-15	A	Frozen	2A	80-100
			15-16	B	Transitional	2B	90-120
			16-18	C	Unfrozen	2C	100-120
	Open larch forest with alder and mountain pine thickets on near-watershed sites (750-1000 m) of windward (northern, northwestern) aspects on gentle slopes	3	15-16	B	Transitional	3B	90-100
			16-18	C	Unfrozen	3C	100-120
	Mountain pine thickets on near-watershed sites (700-1000 m) of windward (northern, northwestern) aspects on gentle slopes	4	9-15	A	Frozen	4A	80-100
			15-16	B	Transitional	4B	90-120
			16-18	C	Unfrozen	4C	100-120
Slope landscapes	Larch forests with pine and mountain pine thickets on gentle slopes (700-900 m) of windward (northern, northwestern) aspects	58	9-15	A	Frozen	58A	<80
	Sparse larch forest with mountain pine thickets on gentle slopes (700-950 m) of windward (northern, northwestern) aspects	59	9-15	A	Frozen	59A	80-100
	Open larch forest with alder and mountain pine thickets on gentle slopes (750-800 m) of windward (northern, northwestern) aspects	60	15-16	B	Transitional	60B	90-120
	Mountain pine thickets on gentle slopes (750-950 m) of windward (northern, northwestern) aspects	61	9-15	A	Frozen	61A	80-100
			15-16	B	Transitional	61B	90-120
			16-18	C	Unfrozen	85C	100-120

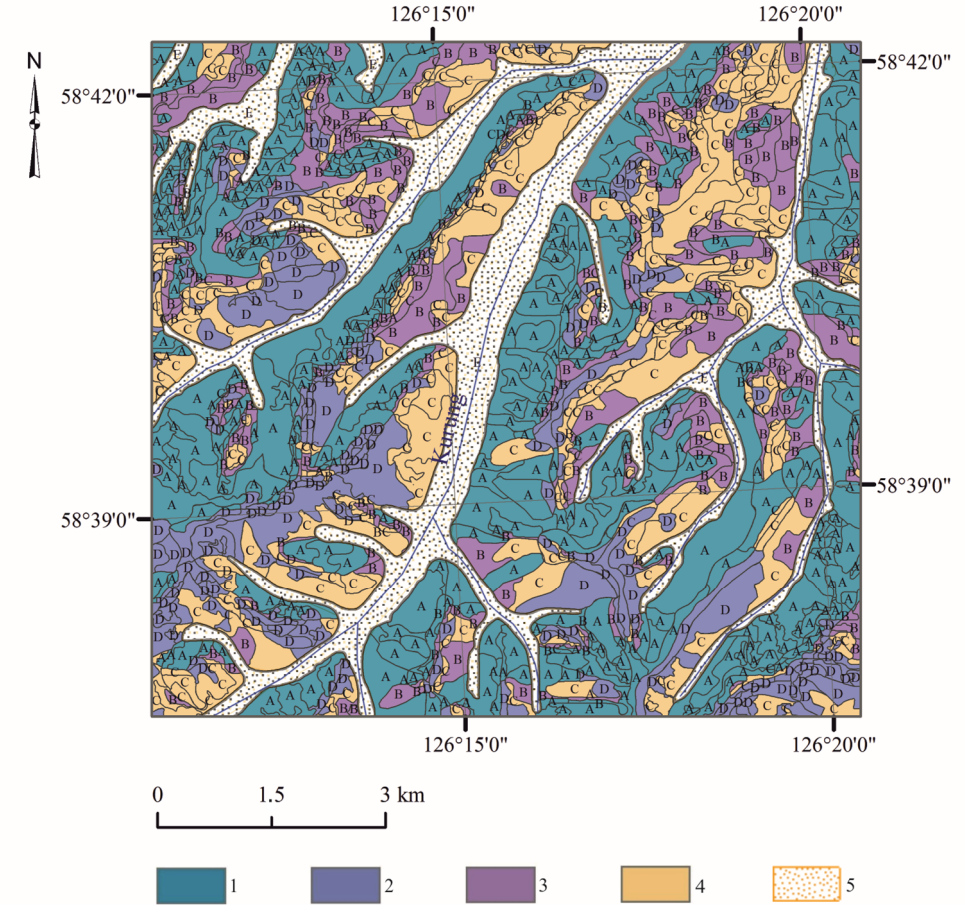

Fig. 4 Map of types of permafrost natural-territorial complexes of the Elkon Massif. 1. permafrost; 2. permafrost of stone fields; 3. ground with temperature of 0°C; 4. unfrozen ground; 5. river valley. Latin letters on the map indicate the condition of the ground given in Table 2.

in Table 2 - ground temperatures increase (from frozen to unfrozen) with increasing snow depth, which is reflected in the LST values. However, as can be seen from Table 2, the condition of the ground is not always related to snow thickness. It should be borne in mind snow cover is not the only factor that controls the thermal condition of the ground. For example, the warming effects of groundwater and infiltrating rainfall, the amount of incoming solar radiation and other local variables that are not visible on satellite images have a significant influence.

The timing of snowmelt also affects the condition of the underlying ground. If snowmelt is delayed, a thick snow cover (100-120 cm or more) can have a cooling effect on the ground. Unfortunately, Landsat satellite imagery can only determine the presence of snow cover in later images, and as for monitoring the thawing stage of snow cover daily, it cannot be made from satellite imagery, due to the fact that Landsat satellite flies once every 16 days.

The new classification unit, "permafrost NTC", obtained by overlaying topography (slope setting, aspect, and slope angle), vegetation, snow cover and LST made it possible to systematize the permafrost component of the landscape (Fig. 4). The derived map and classification provided the following information about the permafrost landscapes in the Elkon Massif.

On the slopes of northern and northwestern exposure, unfrozen ground only occurs on gentle slopes, where vegetation consists of sparse larch forest with mountain-pine thickets or open larch forest with alder and mountain pine and the snow cover is 100 cm or more in thickness, identified by LST=16°C-17°C.

Permafrost on the north- and northwest-facing slopes is present where snow thickness is less than 100 cm. Exceptions to this pattern are areas of stone fields, covered in places with sparse mountain-pine thickets, where snow depths often exceed 100 cm. In areas covered by mountain-pine thickets, late melt of the thick (>100 cm) snow cover can lower the ground temperature. LST for these areas is 9°C-14°C.

Where ground temperatures are at or close to 0°C, the snow cover thickness has intermediate values of 90 to 120 cm; therefore, snow cover thickness is not a reliable indicator for this category. These areas can be identified by LST values of 15°C-16°C.

As noted above, stone fields are associated with high LST values due to strong heating of their surface in summer. However, stone accumulations are not heated on steep and some moderate-angled slopes facing north and northwest, where shading reduces incoming solar radiation, and thus have low LST values similar to frozen ground. It is also worth noting that stone deposits on the gentle and moderate slopes facing north- and northwest are heated less in summer than those on the slopes of other aspects (LST is 15°C-19°C).

The western and northeastern aspects are transitional being in the intermediate position between cold (northern, northwestern) and warm (eastern and southwestern) slopes and have a number of characteristic features. On the northeastern slopes, late June images show snow covering areas of mountain-pine thickets on gentle and moderately-angled surfaces. Also, LST values of 15°C-16°C suggest widespread occurrence of ground with temperatures near 0°C resulting from the low amount of incoming solar radiation and the thick snow cover. The LST of stony deposits on the transitional aspects ranges from 15°C to 26°C. Probably, this is due to the fact that one side of the slopes adjacent to the warm slopes heats up more than the other side adjacent to the cold slopes.

The leeward slopes (eastern, southeastern, southern and southwestern aspects) are characterized by the accumulation of a thick snow cover (especially the east- and southeast-facing slopes). These slopes are predominantly underlain by unfrozen ground, with LST values in the range of 16°C-19°C. Permafrost is present in the middle and lower parts of the slopes where the vegetation cover is larch forest with pine and the snow cover is less than 100 cm thick. Permafrost also occurs below stone fields and is associated with the highest LST values, ranging from 17°C to 26°C.

4 Discussion

The classification (fragment) presented in this article was developed from combined analysis of field-based and remotely sensed data and reflects the level of knowledge and current development of thermal imagery. It demonstrates the applicability of LST to classifying permafrost landscapes and can serve as a starting point for more detailed classifications in future thermal surveys and database development.

This classification using LST is based on the traditional permafrost-landscape classification of Fedorov et al. (2018), however, in view of the fact that

we are investigating only slope and near-watershed landscapes in the altitude interval from 700 to 1200 m, the mapping and classification, respectively, took into account only the eluvial-slopewash, slopewash-colluvial and colluvial stratigraphic-genetic complexes and landscape types characteristic of these sections, as can be seen from section 3.1.

The paper presents new classification solutions taking into account the thickness of the snow cover and LST. The introduction of new criteria for identifying permafrost landscapes will make it possible to differentiate landscapes into frozen and unfrozen in more detail.

From mapping other areas of permafrost distribution, a real example of permafrost-landscape mapping is mapping the distribution of vegetation cover in the permafrost zone of the Qinghai-Tibet Plateau (Wang et al. 2016). In general, the works devoted to the mapping of permafrost in the Qinghai-Tibet Plateau in recent years using the LST parameter are impressive (Zhao et al. 2017; Shi et al. 2018; Li 2019; Zou et al. 2017).

In this study, in addition to a brief overview of the evolution of thermal remote sensing in permafrost, we were faced with the task of reflecting the prospects for using the LST in the research of permafrost in the form of permafrost landscape classification and mapping. The above classification was compiled taking into account the current natural situation. As natural conditions change, the classifications of permafrost landscapes and cartographic generalizations reflecting the actual current state of the natural environment will also change.

5 Conclusions

The review presented in the first part of this article reflects, in general, the development of the method of thermal remote sensing in the study and research of permafrost. The study works of various researchers presented in the article, showing the relationship between the LST and the permafrost, demonstrate the potential of this method for modeling and mapping the spatial distribution of permafrost, as well as understanding the change and development of permafrost in climate warming.

Based on the method of permafrost-landscape mapping using data from 45 wells and Landsat satellite data (including LST), a map of types of permafrost natural-territorial complexes was compiled in ArcGIS, using the example of the territory of the Elkon Massif in Eastern Siberia. The completed map has identified 185 types of permafrost natural-territorial complexes, compiled by a combination of factors such as topography, aspect, surface slope, type of vegetation cover, snow cover depth and LST. The use of the LST parameter made it possible to identify a variety of permafrost/non-permafrost landscapes with specific natural conditions.

The results of the present study showed the possibility of using thermal infrared survey (LST product) in the classification and mapping of landscapes in the permafrost area. This study shows a new approach to the application of LST and can become the starting point for similar studies at the present stage and in the future.

Acknowledgments

We express our gratitude to A.N. Fedorov for help and advice on the classification of permafrost landscapes, to M. N. Zheleznyak and A.R. Kirillin for providing in-situ data on ground temperature and snow cover.

References

Marchenko S, Hachem S, Romanovsky V, Duguay C (2009) Permafrost and active layer modelling in the Northern Eurasia using MODIS Land Surface Temperature as an input data. In: Proceedings of European Geosciences Union General Assembly, Vienna. Vol. 11, p.11077.

Nelson F, Outcalt S (1987) A computational method for prediction and regionalization of permafrost. Arct Alp Res 193: 279-288. https://doi.org/10.1080/00040851.1987.12002602

Hachem S (2009) Using the MODIS Land Surface Temperature Product for Mapping Permafrost: An Application to Northern Quebec and Labrador, Canada. Permafrost Periglacial Process 20: 407-416. https://doi.org/10.1002/ppp.672

Greene J (1971) The application of infrared remote sensing techniques to permafrost - related engineering problems. In: Second Int. symposium on arctic geology (abstr.), San-Francisco. pp 59-61.

Greene J (1972) Application of infrared remote sensing methods to geological and engineering problems of the Arctic. In: 4th Ann. earth resource program rev. Houston, Texas, NASA, MSC. pp 36 (58-1).

Leshack L, Morse F, Brinley W, et al. (1972) Dual-channel airborne I-R scanning for detection of ice in permafrost (Alaska preliminary results). Am Soc Photogr Proc 38: 213-238.

Leshack L, Morse F (1973) Potential use of airborne dual-channel infrared scanning to detect massive ice in permafrost.

North American Contribution Permafrost Second Int. Conf., Washington, D.C. pp 542-549.
Kudryavtsev VA, Garagulya LS, Kondratyeva KA, et al. (1979) Permafrost survey methods. Moscow, Russia: Moscow State University. p 358. (In Russian)
Nekrasov IA (1979) Prospects for the aerospace methods use in geocryology. Aerospace Research of the Earth. M.: Nauka. pp 224-234. (In Russian)
Garbuk SV, Gershenzon VE (1997) Space systems for Earth remote sensing. M.: Publisher A and B. p 296. (In Russian)
Abrams M, Hook S, Ramachandran B (1999) Aster User Handbook, Version 2, NASA/Jet Propulsion Laboratory, Pasadena.
Ihlen V, Zanter K (2019) Landsat 7 (L7) Data Users Handbook,Version 2.0, EROS Sioux Falls, South Dakota.
Kravtsova VI, Baldina EA, Fedorkova YV (2012) The use of satellite images in the thermal infrared range for geographical research (CD-ROM). M.: Moscow State University named after M.V. Lomonosov. (In Russian)
Langer M, Westermann S, Boike J (2010) Spatial and temporal variations of summer surface temperatures of wet polygonal tundra in Siberia - implications for MODIS LST based permafrost monitoring. Remote Sens Environ 114: 2059-2069. https://doi.org/10.1016/j.rse.2010.04.012
Westermann S, Langer M, Boike J (2011) Spatial and temporal variations of summer surface temperatures of high-arctic tundra on Svalbard - Implications for MODIS LST based permafrost monitoring. Remote Sens Environ 115: 908-922. https://doi.org/10.1016/j.rse.2010.11.018
Hachem S, Allard M, Duguay C (2008) A new permafrost map of Quebec-Labrador derived from near-surface temperature data of the Moderate Resolution Imaging Spectroradiometer (MODIS). In: Proceedings of the Ninth International Conference on Permafrost, University of Fairbanks, Fairbanks. pp 591-596.
Hachem S, Duguay C, Allard M (2012) Comparison of MODIS-derived land surface temperatures with near-surface soil and air temperature measurements in continuous permafrost terrain. The Cryosphere 6: 51-69. https://doi.org/10.5194/tc-6-51-2012
Ran Y, Li X, Jin R, Guo J (2015) Remote sensing of the mean annual surface temperature and surface frost number for mapping permafrost in China. Arct Antarc Alp Res 47(2): 255-265. https://doi.org/10.1657/AAAR00C-13-306
Westermann S, Ostby T, Gisnås K, et al. (2015) A ground temperature map of the North Atlantic permafrost region based on remote sensing and reanalysis data. Cryosphere 9: 1303-1319. https://doi.org/10.5194/tc-9-1303-2015
Gisnås K, Etzelmüller B, Farbrot H, et al. (2013) CryoGRID 1.0: Permafrost distribution in Norway estimated by a spatial numerical model. Permafrost Periglacial Process 24: 2-19. https://doi.org/10.1002/ppp.1765
Zhao S, Nan Z, Huang Y, Zhao L (2017) The Application and Evaluation of Simple Permafrost Distribution Models on the Qinghai-Tibet Plateau. Permafrost Periglacial Process 2: 391-404. https://doi.org/10.1002/ppp.1939
Shi Y, Niu F, Yang C, et al. (2018) Permafrost Presence/Absence Mapping of the Qinghai-Tibet Plateau Based on Multi-Source Remote Sensing Data. Remote Sens 10(2): 309. https://doi.org/10.3390/rs10020309
Kornienko SG (2007) Features of using the thermal method for studying and monitoring frozen ground. Drilling and Oil 7-8: 72-75. (In Russian)
Kornienko SG (2012) Methodology for assessing the ice content of frozen ground based on remote sensing data in the visible and infrared range. Exploration of the Earth from Space 5: 75-84. (In Russian)
Medvedkov AA (2016) Cryogenic landscapes mapping based on the analysis of thermal images. Materials of the International Conference "InterCarto/InterGIS; M., Scientific Library. Vol. 1, pp 380-384.
Kalinicheva SV, Fedorov AN, Zhelezniak MN (2019) Mapping mountain permafrost landscapes in Siberia using Landsat thermal imagery. Geosciences 9(1): 4. https://doi.org/10.3390/geosciences9010004
Makarov VS (2017) Spatial distribution of surface radiation temperature in the area of the "Pole of Cold". Questions of the geography of Yakutia. Issue 12: Natural and climatic conditions of North-Eastern Yakutia, Novosibirsk, Science. pp 45-48. (In Russian)
Luo D, Jin H, Marchenko S, Romanovsky V (2018) Difference between near-surface air, land surface and ground surface temperatures and their influences on the frozen ground on the Qinghai-Tibet Plateau. Geoderma 312: 74-85. https://doi.org/10.1016/j.geoderma.2017.09.037
Li A, Xia C, Bao C, Yin G (2019) Using MODIS Land surface temperatures for permafrost thermal modeling in Beiluhe Basin on the Qinghai-Tibet Plateau. Sensors 19(19): 4200. https://doi.org/10.3390/s19194200
Smith M, Riseborough D (2002) Climate and the limit of permafrost: a zonal analysis. Permafrost and Periglacial Processes 13: 1-15. https://doi.org/10.1002/ppp.410
Sazonova TA, Romanovsky V (2003) A model for regional-scale estimation of temporal and spatial variability of active-layer thickness and mean annual ground temperatures. Permafrost Periglacial Process 14(2): 125-140. https://doi.org/10.1002/ppp.449
Jorgenson MT, Romanovsky V, Harden J, et al. (2010) Resilience and vulnerability of permafrost to climate change. Can J For Res 40: 1219-1236. https://doi.org/10.1139/X10-060
Jorgenson MT, Frost GV, Dissing D (2018) Drivers of landscape changes in coastal ecosystems on the Yukon-Kuskokwim Delta, Alaska. Remote Sens 10: 1280. https://doi.org/10.3390/rs10081280
Kokelj SV, Trevor C, Lantz TC, et al. (2017) Climate-driven thaw of permafrost preserved glacial landscapes, northwestern Canada. Geology 45: 371-374. https://doi.org/10.1130/G38626.1
Wang T, Wu T, Wang P, et al. (2019) Spatial distribution and changes of permafrost on the Qinghai-Tibet Plateau revealed by statistical models during the period of 1980 to 2010. Sci. Total Environ 650: 661-670. https://doi.org/10.1016/j.scitotenv.2018.08.398
Fedorov AN (1991) Permafrost Landscapes of Yakutia. Classification and Mapping Issues. Yakutsk, Russia: Permafrost Institute. p 140. (In Russian)
Fedorov AN, Vasilyev NF, Torgovkin YI, et al. (2018) Permafrost-landscape map of the Republic of Sakha (Yakutia) on a Scale 1:1,500,000. Geosciences 8(12): 465. https://doi.org/10.3390/geosciences8120465
Sochava VB (1978) Introduction to the doctrine of geosystems. Novosibirsk: Nauka. p 318. (In Russian)
Wang ZW, Wang Q, Zhao L, et al. (2016) Mapping the vegetation distribution of the permafrost zone on the Qinghai-Tibet Plateau. J Mt Sci 13: 1035-1046. https://doi.org/10.1007/s11629-015-3485-y
Zou D, Zhao L, Sheng Y, et al. (2017) A new map of permafrost distribution on the Tibetan Plateau. Cryosphere 11: 2527-2542. https://doi.org/10.5194/tc-11-2527-2017